



Published in final edited form as:

Biochem Biophys Res Commun. 2015 September 25; 465(3): 338–343. doi:10.1016/j.bbrc.2015.07.142.

Intracellular Distribution of TM4SF1 and Internalization of TM4SF1-antibody Complex in Vascular Endothelial Cells

Tracey E. Sciuto¹, Anne Merley¹, Chi-lou Lin¹, Douglas Richardson², Yu Liu³, Dan Li¹, Ann M. Dvorak¹, Harold F. Dvorak^{1,*}, and Shou-Ching S. Jaminet^{1,*}

¹Center for Vascular Biology Research and Department of Pathology, Beth Israel Deaconess Medical Center and Harvard Medical School

²Department of Molecular and Cellular Biology, Harvard University

³Department of Pharmacology, Shanxi Medical University, Xinjiannanlu 56, Shanxi Province, Taiyuan 030001, China

Abstract

Transmembrane-4 L-six family member-1 (TM4SF1) is a small plasma membrane-associated glycoprotein that is highly and selectively expressed on the plasma membranes of tumor cells, cultured endothelial cells, and, *in vivo*, on tumor-associated endothelium. Immunofluorescence microscopy also demonstrated TM4SF1 in cytoplasm and, tentatively, within nuclei. With monoclonal antibody 8G4, and the finer resolution afforded by immuno-nanogold transmission electron microscopy, we now demonstrate TM4SF1 in uncoated cytoplasmic vesicles, nuclear pores and nucleoplasm. Because of its prominent surface location on tumor cells and tumor-associated endothelium, TM4SF1 has potential as a dual therapeutic target using an antibody drug conjugate (ADC) approach. For ADC to be successful, antibodies reacting with cell surface antigens must be internalized for delivery of associated toxins to intracellular targets. We now report that 8G4 is efficiently taken up into cultured endothelial cells by uncoated vesicles in a dynamin-dependent, clathrin-independent manner. It is then transported along microtubules through the cytoplasm and passes through nuclear pores into the nucleus. These findings validate TM4SF1 as an attractive candidate for cancer therapy with antibody-bound toxins that have the capacity to react with either cytoplasmic or nuclear targets in tumor cells or tumor-associated vascular endothelium.

*Corresponding authors: Shou-Ching S. Jaminet and Harold F. Dvorak, Department of Pathology, Beth Israel Deaconess Medical Center, 330 Brookline Avenue, RN-280D, Boston, MA02215, USA. Telephone and sjaminet@bidmc.harvard.edu (617-667-8156); hdvorak@bidmc.harvard.edu (617-667-8529); Fax: 617-667-3591.

Publisher's Disclaimer: This is a PDF file of an unedited manuscript that has been accepted for publication. As a service to our customers we are providing this early version of the manuscript. The manuscript will undergo copyediting, typesetting, and review of the resulting proof before it is published in its final citable form. Please note that during the production process errors may be discovered which could affect the content, and all legal disclaimers that apply to the journal pertain.

Conflicts of interests

The authors have declared that no competing interests exist.

Appendix A. Supplementary data

Keywords

TM4SF1; endothelial cells; antibody internalization; microtubules; antibody drug conjugate

1. Introduction

Transmembrane-4 L-six family member-1 (TM4SF1) is a small plasma membrane glycoprotein with tetraspanin topology [1]. It was originally described as a tumor cell antigen [2] and was later found to be expressed at low levels on normal vascular endothelium [3]. Subsequently, we demonstrated that TM4SF1 is highly expressed by cultured blood and lymphatic endothelial cells (EC), and, *in vivo*, by the endothelium lining angiogenic blood vessels [4,5]. TM4SF1 is clustered in intermittent microdomains called TMED (TM4SF1-enriched microdomains) on plasma membrane and on nanopodia, which are thin, elongate projections that extend for up to 50 μm from the EC surface [4,5,6]. In addition to its distribution on the cell surface, immunofluorescence microscopy also demonstrated TM4SF1 deposits in the cytoplasm, and, tentatively, in nuclei of both cultured EC and tumor cells [4,5,6]. TM4SF1 has been shown to regulate tumor cell growth, motility, and metastasis [1,2,7]. Knockdown of TM4SF1 rendered EC unable to polarize and restricted their migration and proliferation *in vitro* and their capacity to form new blood vessel *in vivo* [4,5].

The restriction of high TM4SF1 expression to the surface of many tumor cells and tumor-associated vascular EC suggested its potential as a dual therapeutic target [4,5]. We reported earlier that 8G4, a mouse anti-human TM4SF1 monoclonal antibody, effectively destroyed a human vascular network that we had engineered in Matrigel plugs implanted in nude mice, along with the human tumor cells that this vascular network supported [8], presumably acting by antibody-dependent cell-mediated cytotoxicity (ADCC) or complement-dependent cytotoxicity (CDC). However, ADCC and CDC are relatively inefficient processes with inherent, immune-associated risks that limit their utility [9]. In recent years antibody drug conjugates (ADC) have shown promise as a new approach to cancer treatment [10], and we recently reported that anti-TM4SF1 antibodies conjugated with the auristatin cytotoxin mc-3377 strikingly regressed TM4SF1-expressing human tumor xenografts [11]. To be successful, ADC requires that the antibody-toxin complex be internalized so that the toxin can react with intracellular targets, e.g., tubulin in the case of mc-3377.

The studies reported here had two goals. The first was to better define the subcellular distribution of TM4SF1 in cultured EC, and, for comparison, in the endothelium of angiogenic blood vessels supplying a human cancer. The second goal was to demonstrate and determine the mechanisms of anti-TM4SF1 antibody uptake, an essential first step if ADC is to be useful in cancer therapy.

2. Methods

2.1. Cell culture and inhibitors

Human umbilical vein endothelial cells (HUVEC) from Lonza (Walkersville, MD) were cultured in EGM2-MV medium, and used at passage 4–5. The following inhibitors were from Abcam (Cambridge, MA): pitstop-2 (clathrin inhibitor), chlorpromazine (an inhibitor of clathrin and caveolin mediated endocytosis), bifilomycin A (autophagy Inhibitor), and dynasore (dynamain inhibitor).

2.2. Immunostaining

Experimental procedures were described in detail previously [6]. Briefly, cells and tissue sections were fixed with 4% paraformaldehyde, washed in PBS, and blocked with PBS/2% FBS prior to immunostaining with primary antibodies 8G4 (mouse anti-human TM4SF1, IgG1 isotype) [8] or rat anti-human α -tubulin (Santa Cruz Biotechnology, Santa Cruz, CA), followed by secondary donkey anti-mouse (or anti-rat) Alexa Fluor-488 or -594 labeled antibodies (Life technology, Carlsbad, CA). Phalloidin-TRIC and mouse IgG1 were purchased from Sigma (St. Louis, MO). Nikon TE-300 was used to capture epifluorescence images and a Zeiss ELYRA PS1 super resolution microscope for Structure Illumination Microscopy (Harvard Center for Biological Imaging).

Transmission electron-microscopy was performed on HUVEC fixed and immunostained with 8G4 as above, followed by a secondary goat anti-mouse Fab'-labeled with both Alexa Fluor-488 and nanogold (1.4 nm gold particles, Nanoprobes, Yaphank, NY) as described [5]. A resected gastric adenocarcinoma was similarly fixed and prepared for electron microscopic study with permission from the BIDMC IRB. All immunocytochemistry images were representative selections from at least three separate experiments.

2.3. Flow Cytometry

HUVEC were harvested after light trypsinization, washed in cold PBS, suspended in 1 ml cold blocking buffer (PBS/1% FBS) that contained 1 μ g first antibody [8G4, mouse anti-human E-selectin antibody (IgG1 subtype) from Novus (Littleton, CO), or mouse IgG1], and incubated on ice for 1h with occasional agitation. Cells were then centrifuged (500xg, 5 min), washed 3x with cold PBS, incubated with 100 ng/ml second antibody (Alexa-488 labeled donkey anti-mouse IgG, Life Technology), and washed 3x with cold PBS. Cell suspensions were analyzed with FACScan (Becton Dickinson, San Jose CA). 10^4 events were collected for each analysis. All flow cytometry histograms were representative selections from at least three separate experiments

2.4. Cell fractionation, immunoprecipitation and immunoblotting

HUVEC were grown to 80–90% confluency, suspended as above, and fractionated into their subcellular compartments using kits from Thermo Scientific (Logan, UT). The following antibodies (Cell Signaling, Danvers, MA) were used to define different subcellular fractions: rabbit anti-human HDAC2 (nuclear protein), rabbit anti-human histone-H3 (nuclear chromatin), and mouse anti-human vimentin (cytoskeleton). HRP-conjugated goat anti-rabbit and goat anti-mouse antibodies (Cell Signaling) served as secondary antibodies.

For TM4SF1 pull-down assays, suspended HUVEC were pre-incubated with 8G4 or with an isotype-matched mouse IgG1 control antibody for 1 hour on ice, washed 3x with PBS to remove unbound antibody, and returned to culture for 4h at 37°C before cells were harvested for total protein extraction in a cell lysis buffer comprised of Tris-buffered saline (TBS), pH 7.0, protease/phosphatase inhibitor cocktails, and 0.1% Triton X-100 (Life Technology). Protein-G beads were then added to the lysates to pull down 8G4 (or control IgG). The 8G4 pull down fraction was then electrophoresed and immunoblotted with 8G4 that had been conjugated with HRP (Life Technology labeling kit).

3. Results

3.1. Subcellular distribution of TM4SF1 in human umbilical vein endothelial cells (HUVEC) and in the microvascular EC of human gastric adenocarcinoma

Initial studies were performed to define TM4SF1's subcellular distribution within cultured endothelial cells more precisely than was possible with immunofluorescence microscopy. Using immuno-nanogold transmission electron microscopy with 8G4, a monoclonal antibody specific for human TM4SF1, we found that TM4SF1 clusters (TMED) were distributed on the plasma membrane (blue arrows) and on the membranes of uncoated cytoplasmic vesicles (yellow circles), some of which were attached to the plasma membrane (Fig. 1Ab). In addition, individual gold particles were found on the nuclear membrane and in nuclear pores (red arrows) and were also scattered in the nucleoplasm (red circles). Gold particles were additionally found in association with the rough endoplasmic reticulum, indicative of new TM4SF1 synthesis (Fig. 1Ac). An isotype-matched mouse IgG1 which served as a negative control did not exhibit labeling (data not shown).

Using the same immuno-nanogold technology, we determined that TM4SF1 had an identical surface, cytoplasmic and nuclear distribution *in vivo* in the EC lining angiogenic microvessels that supplied a resected adenocarcinoma of the stomach (Fig. 1Ba). The luminal surface of the endothelium demonstrated much stronger labeling than the abluminal surface (Fig. 1Bb). Only rare gold particles were found on EC distant from the tumor (Supplementary Figure S1).

Subcellular fractionation of cultured HUVEC, followed by immunoblotting, extended these morphological findings (Supplementary Figure S2). 8G4, as well as several commercial anti-TM4SF1 antibodies [5], demonstrated three bands of 28-, 25- and 22-kD in the cell membrane and soluble nuclear fractions, but only the 28-kD band was present in the cytoskeletal and nuclear chromatin fractions. The significance of the three bands that react with 8G4 and other anti-TM4SF1 antibodies is not known and could reflect incomplete processing or degradation of TM4SF1. TM4SF1 was not detected in the soluble cytosolic fraction.

3.2. Internalization of 8G4 in HUVEC

To determine whether TM4SF1 was internalized following reaction with antibody, we exposed HUVEC to 8G4 for 1h at 4°C and then returned them to culture. Flow cytometry demonstrated a progressively increasing loss of 8G4 signal from the cell surface: 20.8%,

52.2%, and 95%, at 2, 4, and 24h, respectively (Supplementary Figure S3A). Similar rates of cell surface signal loss was seen in six other mouse anti-human TM4SF1 antibodies [8] studied (data not shown). While some of this loss could reflect shedding from the cell surface, immunofluorescence microscopy demonstrated substantial 8G4 uptake in the cytoplasm and over the nucleus (Fig. 2A); intracellular 8G4 staining reached a peak at 4h and was largely lost by 24h. Individual frames of Z-stacked confocal images (Supplementary Figure S3B) also demonstrated internalized 8G4 at 4h in the cytoplasm (frame-15, yellow arrows) and definitively in the nucleus (frame-6, white arrows). Control, isotype-matched mouse IgG1 antibody did not bind to HUVEC as determined by flow cytometry (Supplementary Figure S3A) and immunocytochemistry (not shown).

Immuno-nanogold transmission electron microscopy provided more detailed evidence of 8G4 uptake (Fig. 2B). HUVEC were reacted with 8G4 and returned to culture as above. At 4h, large clusters of nanogold particles were found in association with uncoated cytoplasmic vesicles (yellow circles), some of which were attached to the plasma membrane. Additional labeling was associated with the nuclear membrane and nuclear pores (red arrows) and smaller clusters and individual particles were found within the nucleoplasm (red circles). Gold clusters in the cytoplasm and on the nuclear membrane were consistently larger than those visualized in the same locations by 8G4 staining of fixed tissue sections (compare Fig. 2B with Figs. 1A and B).

To determine whether TM4SF1 was internalized along with 8G4, HUVEC were lysed at the 4h time point when 8G4 accumulation was maximal. We then pulled down 8G4 from lysed cells with protein-G beads, and demonstrated 28kD TM4SF1 in the pull-down fraction by immunoblotting (Fig. 2C). Consistent with the localization of ingested 8G4 to *uncoated* cytoplasmic vesicles, we did not demonstrate clathrin in the 8G4 pull-down fraction (data not shown).

3.3. 8G4-TM4SF1 internalization requires dynamin but not clathrin

To elucidate the mechanisms of uptake of the 8G4-TM4SF1 complex we quantified the loss of intensity of cell surface-bound 8G4 by flow cytometry in the presence or absence of inhibitors. Intensity of cell surface 8G4 staining measured $96.4 \pm 2.1\%$ after 1h exposure of HUVEC to 8G4 at 4°C ; in the absence of drug treatment, that percentage had fallen to $37.8 \pm 6.5\%$ at 4h of culture at 37°C . Similar levels were found for cells cultured with several different drugs: $39.1 \pm 3.2\%$ for cells treated with pitstop-2 (a clathrin inhibitor); $47.1 \pm 3.5\%$ for treatment with chlorpromazine (an inhibitor of clathrin and caveolae mediated endocytosis); and $38.9 \pm 4.9\%$ for treatment with bafilomycin A (an autophagy inhibitor). However, in cells cultured with dynasore, a dynamin inhibitor, the decline in staining intensity was almost entirely prevented as $90.1 \pm 1.7\%$ of cell surface signal intensity was retained on the cell surface at 4h.

Immunofluorescence microscopy provided supportive evidence that dynasore, but not the other inhibitors, prevented 8G4 uptake. Immediately after reaction with HUVEC, and prior to reattachment to culture matrix, cells were rounded, and as expected, 8G4 was confined to the plasma membrane (Fig. 3A). Subsequently, surface signal intensity decreased and intracellular staining increased progressively in the absence of inhibitors, and, to an

equivalent extent, in cells exposed to pitstop-2, chlorpromazine, and bifilomycin A (Fig. 3B–E). However, 8G4 signal remained strong and predominantly on the cell surface of HUVEC cultured with dynasore (Fig. 3F). Similar kinetics of 8G4-TM4SF1 uptake were observed in several human TM4SF1-expressing tumor cell lines (data not shown), indicating that TM4SF1 uptake is not cell-type specific.

The flow cytometry and immunofluorescence data indicate much slower internalization kinetics for 8G4 than that reported for antibodies reactive with other cell surface proteins, such as the tetraspanin CD63 [12] and E-selectin [13], that are taken up by a clathrin-mediated mechanism. To validate our methodology and findings with 8G4, we reacted HUVEC with an antibody against E-selectin and evaluated its loss from the cell surface over time. Consistent with the findings of others [14], and in contrast to 8G4 (37.8±6.5% of cell surface retention at 4h), an antibody specific for E-selectin was entirely cleared from the surface of HUVEC within 1h (Supplementary Figure S4).

3.4. TM4SF1 internalization along microtubules

Motor proteins provide the driving force behind most cytoplasmic transport of proteins and vesicles [15], and microtubules have been shown to serve as “railroad tracks” that guide their movement [16]. We previously demonstrated that TM4SF1 interacted with myosin-X (Myo10) [5], a motor protein that binds microtubules through a C-terminal MyTH4-FERM domain cassette [17,18,19]. We therefore used confocal microscopy to look for an association between internalized 8G4, presumably complexed to TM4SF1, and microtubules. As shown in Fig. 4A, internalized 8G4 was associated with α -tubulin-stained microtubules (inset i, white arrows) at 4h and Structural Illumination Microscopy confirmed this association elegantly (Fig. 4B).

4. Discussion

The data presented here demonstrate that TM4SF1 has an identical subcellular distribution in cultured HUVEC and in the endothelium of newly formed blood vessels supplying a resected gastric adenocarcinoma (Fig. 1). In both cases TM4SF1 was found not only on the plasma membrane but also in association with uncoated cytoplasmic vesicles and in nuclear pores and nucleoplasm. The data also show that an anti-TM4SF1 antibody, 8G4, was efficiently internalized in HUVEC by means of uncoated vesicles in a dynamin-dependent, clathrin-independent fashion; once internalized, 8G4 was carried along microtubules through the cytoplasm and passed through nuclear pores into the nucleus. These findings validate TM4SF1 as an attractive candidate for cancer therapy with antibody-associated toxins that have the capacity to react with either cytoplasmic or nuclear targets.

Many surface proteins (e.g., CD63 [12], E-selectin [13], prostate-specific membrane antigen [20], receptor tyrosine kinases [21]) are internalized by clathrin-dependent mechanisms. However, we found no role for clathrin in 8G4 internalization. 8G4 was localized to uncoated (i.e., clathrin-negative) cytoplasmic vesicles (Fig. 2B), and the 8G4-TM4SF1 complex was internalized much more slowly than is typical of clathrin-requiring proteins such as E-selectin (compare Supplementary Figure S3A with S4) [13,14]. Further, clathrin-mediated endocytosis is initiated through the concerted action of the clathrin coat protein

and adaptor proteins that selectively recruit transmembrane proteins for cell uptake [22]. TM4SF1's three short intracellular domains (intracellular loop and the N- and C-termini) lack the [DE]xxxL[LI] or [FY]xNPx[YF] recognition motifs [22,23] for clathrin adaptor proteins. Finally, 8G4-TM4SF1 uptake was not prevented by clathrin inhibitors (Fig. 3), and 8G4-TM4SF1 complexes were unable to pull down clathrin (data not shown).

However, 8G4 internalization was dependent on dynamin, as determined by the finding that dynasore, a dynamin inhibitor, strikingly reduced 8G4 uptake (Fig. 3F). Dynamin is a large (100-kD), microtubule-associated GTPase that forms a helical polymer around the constricted necks of vesicles, and, upon GTP hydrolysis, mediates fission of vesicles from the plasma membrane [23,24]. Dynamin is involved in many types of endocytosis that involve vesicle scission, including clathrin-mediated endocytosis [23,24], but also, as illustrated here, that of uncoated, caveolae-like vesicles (Fig. 2B). Once internalized, 8G4 remained attached to TM4SF1, as demonstrated by 8G4 pull downs which included TM4SF1 (Fig. 2C) as well as dynamin (not shown); dynamin pull-downs also contained TM4SF1 (data not shown). Internalized 8G4 attached to microtubules for transport through the cytoplasm. Association of 8G4 with microtubules may be mediated through TM4SF1 which can bind myosin-X, a phosphoinositide-binding motor myosin that binds α -tubulin via its C-terminal MyTH4-FERM domain cassette [19].

8G4 lost its association with vesicle membranes as it passed through nuclear pores and entered the nucleoplasm. Entry of 8G4 into the nucleoplasm (Fig. 2A, 2Ba; Supplementary Figure S3B) was unexpected, as all three short cytosolic domains of TM4SF1 lack nuclear localization signals [25]. As far as is known, antibodies such as 8G4 also lack such signals. One possibility is that, having entered the cytoplasm, TM4SF1 diffused into the nucleus. This is possible because molecules smaller than ~40 kDa can passively diffuse through the nuclear pore and TM4SF1's largest isoform is 28-kD (Supplementary Figure S2). However, most proteins enter the nucleus by an active, carrier-mediated transport system [26]. What such a carrier might be in the case of anti-TM4SF1 antibodies is a matter of speculation. Proteins known to form complexes with TM4SF1, including myosin-X and β -actin [4,5], lack nuclear pore signals [27,28], as does microtubule α -tubulin along which the 8G4-TM4SF1 complex tracks through the cytoplasm (Fig. 4). Whatever the mechanism, our findings validate TM4SF1 as a candidate for ADC cancer therapy with toxins against nuclear as well as cytoplasmic targets.

Supplementary Material

Refer to Web version on PubMed Central for supplementary material.

Acknowledgement

We thank Kelly Seldi for help capturing confocal images, the Harvard Center for Biological Imaging for infrastructure and support. This work was supported by NIH grant P01 CA92644, by SIG award RR1S1027990, and by a contract from the National Foundation for Cancer Research.

References

1. Wright MD, Ni J, Rudy GB. The L6 membrane proteins--a new four-transmembrane superfamily. *Protein Sci.* 2000; 9:1594–1600. [PubMed: 10975581]
2. Hellstrom I, Horn D, Linsley P, Brown JP, Brankovan V, Hellstrom KE. Monoclonal mouse antibodies raised against human lung carcinoma. *Cancer Res.* 1986; 46:3917–3923. [PubMed: 3731064]
3. DeNardo SJ, O'Grady LF, Macey DJ, Kroger LA, DeNardo GL, Lamborn KR, Levy NB, Mills SL, Hellstrom I, Hellstrom KE. Quantitative imaging of mouse L-6 monoclonal antibody in breast cancer patients to develop a therapeutic strategy. *Int J Rad Appl Instrum B.* 1991; 18:621–631. [PubMed: 1743985]
4. Shih SC, Zukauskas A, Li D, Liu G, Ang LH, Nagy JA, Brown LF, Dvorak HF. The L6 protein TM4SF1 is critical for endothelial cell function and tumor angiogenesis. *Cancer Res.* 2009; 69:3272–3277. [PubMed: 19351819]
5. Zukauskas A, Merley A, Li D, Ang LH, Sciuto TE, Salman S, Dvorak AM, Dvorak HF, Jaminet SC. TM4SF1: a tetraspanin-like protein necessary for nanopodia formation and endothelial cell migration. *Angiogenesis.* 2011; 14:345–354. [PubMed: 21626280]
6. Lin CI, Lau CY, Li D, Jaminet SC. Nanopodia--thin, fragile membrane projections with roles in cell movement and intercellular interactions. *J Vis Exp.* 2014:e51320.
7. Kao YR, Shih JY, Wen WC, Ko YP, Chen BM, Chan YL, Chu YW, Yang PC, Wu CW, Roffler SR. Tumor-associated antigen L6 and the invasion of human lung cancer cells. *Clin Cancer Res.* 2003; 9:2807–2816. [PubMed: 12855661]
8. Lin CI, Merley A, Sciuto TE, Li D, Melero-Martin JM, Dvorak AM, Dvorak HF, Jaminet SC. TM4SF1: a new vascular therapeutic target in cancer. *Angiogenesis.* 2014; 17:897–907. [PubMed: 24986520]
9. Brennan FR, Morton LD, Spindeldreher S, Kiessling A, Allenspach R, Hey A, Muller PY, Frings W, Sims J. Safety and immunotoxicity assessment of immunomodulatory monoclonal antibodies. *MAbs.* 2010; 2:233–255. [PubMed: 20421713]
10. Sassoon I, Blanc V. Antibody-drug conjugate (ADC) clinical pipeline: a review. *Methods Mol Biol.* 2013; 1045:1–27. [PubMed: 23913138]
11. Visintin A, Knowlton K, Tyminski E, Lin CI, Zheng X, Marquette K, Jain S, Tchistiakova L, Li D, O'Donnell CJ, Maderna A, Cao X, Dunn R, Snyder W, Abraham AK, Leal M, Shetty S, Barry A, Zawel L, Coyle AJ, Dvorak HF, Jaminet SC. Novel Anti-TM4SF1 Antibody Drug Conjugates with Activity against Tumor Cells and Tumor Vasculature. *Mol Cancer Ther.* 2015; 14:1868–1876. [PubMed: 26089370]
12. Pols MS, Klumperman J. Trafficking and function of the tetraspanin CD63. *Exp Cell Res.* 2009; 315:1584–1592. [PubMed: 18930046]
13. Setiadi H, McEver RP. Clustering endothelial E-selectin in clathrin-coated pits and lipid rafts enhances leukocyte adhesion under flow. *Blood.* 2008; 111:1989–1998. [PubMed: 18029551]
14. von Asmuth EJ, Smeets EF, Ginsel LA, Onderwater JJ, Leeuwenberg JF, Buurman WA. Evidence for endocytosis of E-selectin in human endothelial cells. *Eur J Immunol.* 1992; 22:2519–2526. [PubMed: 1382989]
15. Mallik R, Gross SP. Molecular motors: strategies to get along. *Curr Biol.* 2004; 14:R971–R982. [PubMed: 15556858]
16. Leopold PL, Pfister KK. Viral strategies for intracellular trafficking: motors and microtubules. *Traffic.* 2006; 7:516–523. [PubMed: 16643275]
17. Woolner S, O'Brien LL, Wiese C, Bement WM. Myosin-10 and actin filaments are essential for mitotic spindle function. *J Cell Biol.* 2008; 182:77–88. [PubMed: 18606852]
18. Zhang H, Berg JS, Li Z, Wang Y, Lang P, Sousa AD, Bhaskar A, Cheney RE, Stromblad S. Myosin-X provides a motor-based link between integrins and the cytoskeleton. *Nat Cell Biol.* 2004; 6:523–531. [PubMed: 15156152]
19. Hirano Y, Hatano T, Takahashi A, Toriyama M, Inagaki N, Hakoshima T. Structural basis of cargo recognition by the myosin-X MyTH4-FERM domain. *Embo J.* 2011; 30:2734–2747. [PubMed: 21642953]

20. Liu H, Rajasekaran AK, Moy P, Xia Y, Kim S, Navarro V, Rahmati R, Bander NH. Constitutive and antibody-induced internalization of prostate-specific membrane antigen. *Cancer Res.* 1998; 58:4055–4060. [PubMed: 9751609]
21. Goh LK, Sorkin A. Endocytosis of receptor tyrosine kinases. *Cold Spring Harb Perspect Biol.* 2013; 5:a017459. [PubMed: 23637288]
22. Kelly BT, Owen DJ. Endocytic sorting of transmembrane protein cargo. *Curr Opin Cell Biol.* 2011; 23:404–412. [PubMed: 21450449]
23. Doherty GJ, McMahon HT. Mechanisms of endocytosis. *Annu Rev Biochem.* 2009; 78:857–902. [PubMed: 19317650]
24. Roux A, Uyhazi K, Frost A, De Camilli P. GTP-dependent twisting of dynamin implicates constriction and tension in membrane fission. *Nature.* 2006; 441:528–531. [PubMed: 16648839]
25. Marken JS, Schieven GL, Hellstrom I, Hellstrom KE, Aruffo A. Cloning and expression of the tumor-associated antigen L6. *Proc Natl Acad Sci U S A.* 1992; 89:3503–3507. [PubMed: 1565644]
26. Marfori M, Mynott A, Ellis JJ, Mehdi AM, Saunders NF, Curmi PM, Forwood JK, Boden M, Kobe B. Molecular basis for specificity of nuclear import and prediction of nuclear localization. *Biochim Biophys Acta.* 2011; 1813:1562–1577. [PubMed: 20977914]
27. Spencer VA. Nuclear actin: A key player in extracellular matrix-nucleus communication. *Commun Integr Biol.* 2011; 4:511–512. [PubMed: 22046450]
28. de Lanerolle P, Serebryanny L. Nuclear actin and myosins: life without filaments. *Nat Cell Biol.* 2011; 13:1282–1288. [PubMed: 22048410]

Highlights

- Anti-TM4SF1 antibody 8G4 was efficiently taken up by cultured endothelial cells
- TM4SF1-8G4 internalization is dynamin-dependent but clathrin-independent
- TM4SF1-8G4 complexes internalize along microtubules to reach the perinuclear region
- Internalized TM4SF1-8G4 complexes pass through nuclear pores into the nucleus
- TM4SF1 is an attractive candidate for ADC cancer therapy

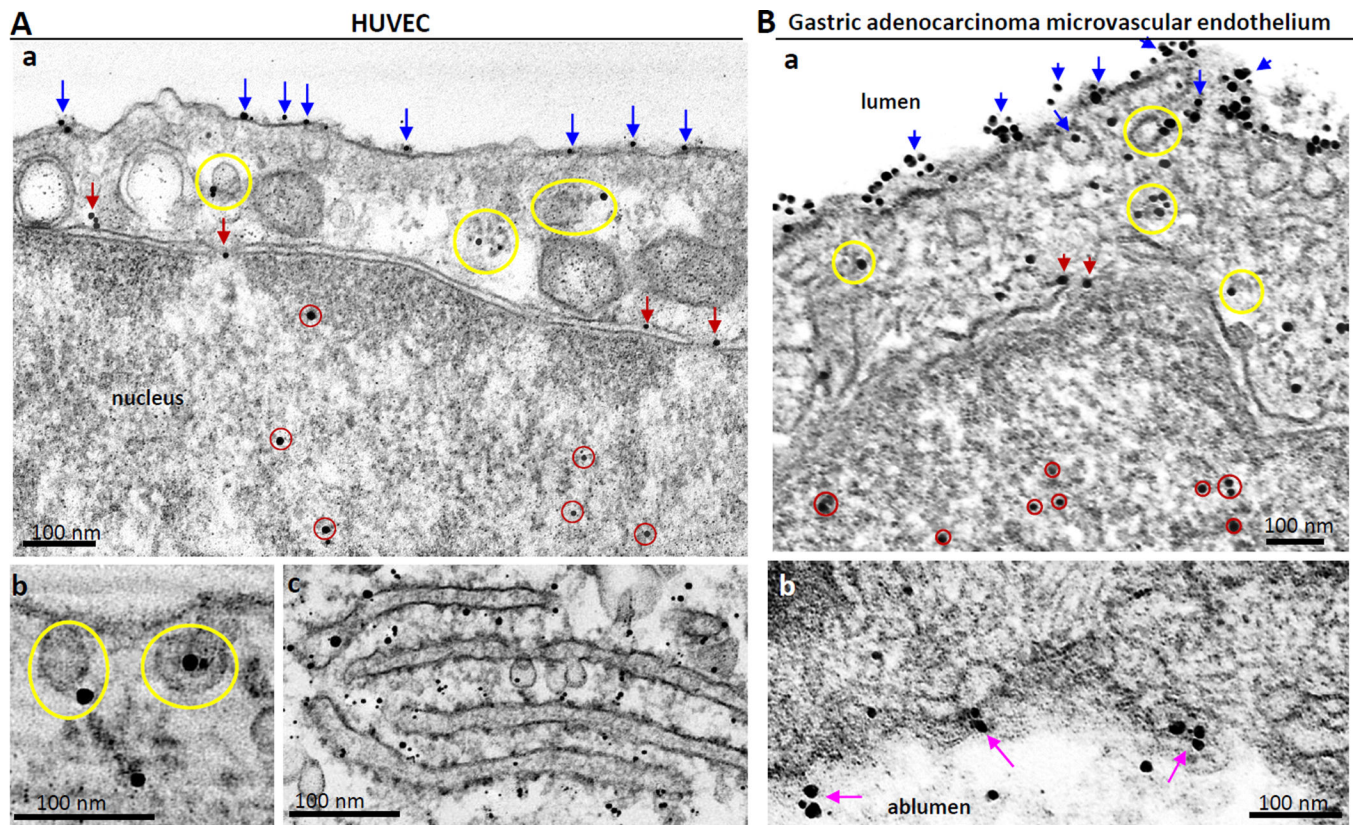


Fig. 1. Distribution of TM4SF1 in HUVEC (A) and in human gastric cancer vascular endothelial cells (B) as determined by immuno-nanogold transmission electron microscopy. HUVEC cultured on glass discs and a resected gastric adenocarcinoma and immunostained with mouse anti-human TM4SF1 antibody 8G4, followed by nanogold labeled anti-mouse IgG1. (Aa,b) Nanogold deposits localized TM4SF1 in HUVEC to the plasma membrane (blue arrows), cytoplasmic vesicles (yellow circles), nuclear membrane and nuclear pores (red arrows), and the nucleoplasm (red circles). (Ac) Rough endoplasmic reticulum demonstrates extensive nanogold labeling. (Ba,b) TM4SF1 labeling of human gastric cancer vascular endothelial cells is similar to that in HUVEC. Luminal membrane staining (Ba) is much stronger than that of albuminal labeling (Bb, pink arrows). Scale bars, 100 nm.

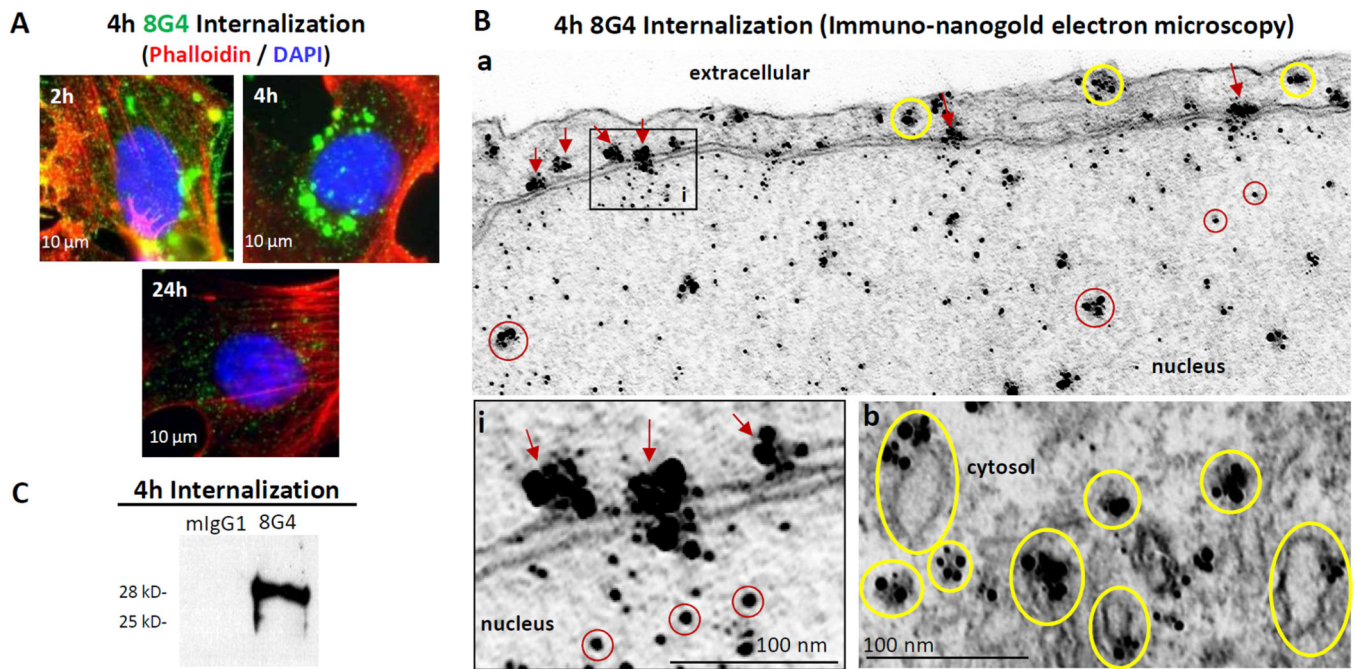
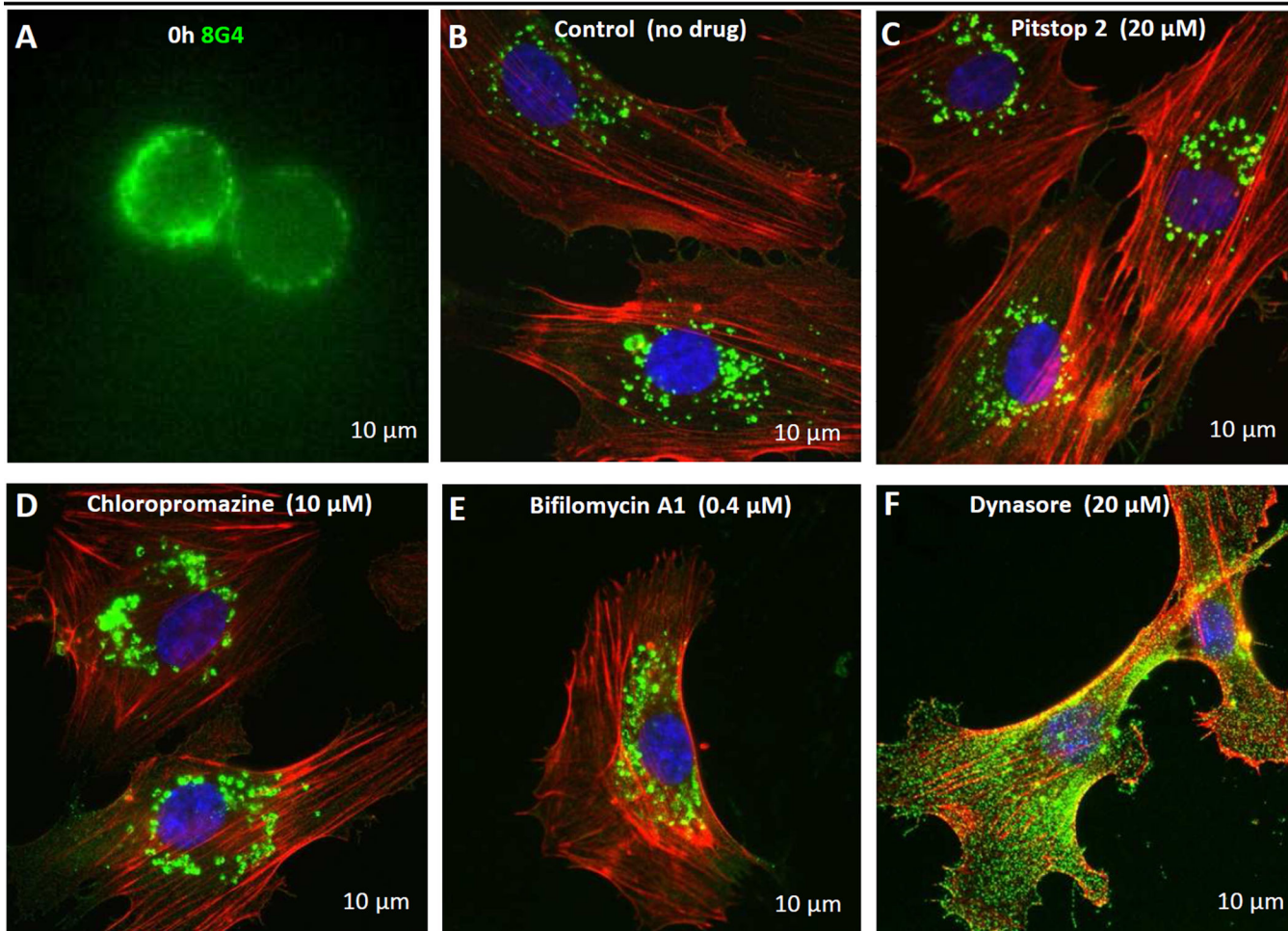


Fig. 2. Internalization of anti-TM4SF1 monoclonal antibody 8G4 in HUVEC. HUVEC were incubated with 8G4 or with control mouse-IgG1 (mIgG1) for 1h at 4°C, washed, and returned to culture at 37° C for varying periods of time to follow 8G4 uptake by (A) immunofluorescence microscopy, (B) immuno-nanogold transmission electron microscopy, and (C) immunoblotting. (A) 8G4 achieved maximal intensity in cytoplasm and nucleus at 4h and was largely lost at 24h. (B) At 4h, gold particles are demonstrated in the cytoplasm (yellow circles), associated with the nuclear membrane and nuclear pores (red arrows) and within the nucleoplasm (red circles). (C) Immunoblot of 8G4 pull down prepared 4h after returning HUVEC to culture demonstrates 28-kD form of TM4SF1.

4h 8G4 Internalization (Phalloidin/DAPI)

**Fig. 3.**

Internalization of TM4SF1 in HUVEC in the presence of different inhibitors. HUVEC were pre-labeled with 8G4 at 4°C (A) and returned to culture at 37°C without (B) or in the presence of the following inhibitors: (C) 20 μM pitstop-2 (clathrin inhibitor), (D) 10 μM chlorpromazine (clathrin and caveolin mediated endocytosis inhibitor), (E) 0.4 μM bafilomycin A (autophagy inhibitor), or (F) 20 μM dynasore (dynamin inhibitor). After 4h, cells were fixed in 4% paraformaldehyde. Immunocytochemistry demonstrates substantial and equivalent 8G4 uptake at 4h with no added inhibitor or in the presence of pitstop-2, chlorpromazine, or bafilomycin A. However, 8G4 remained largely on the cell surface when cultured with dynasore.

co-localization of internalized 8G4 and Tubulin in HUVEC (DAPI)

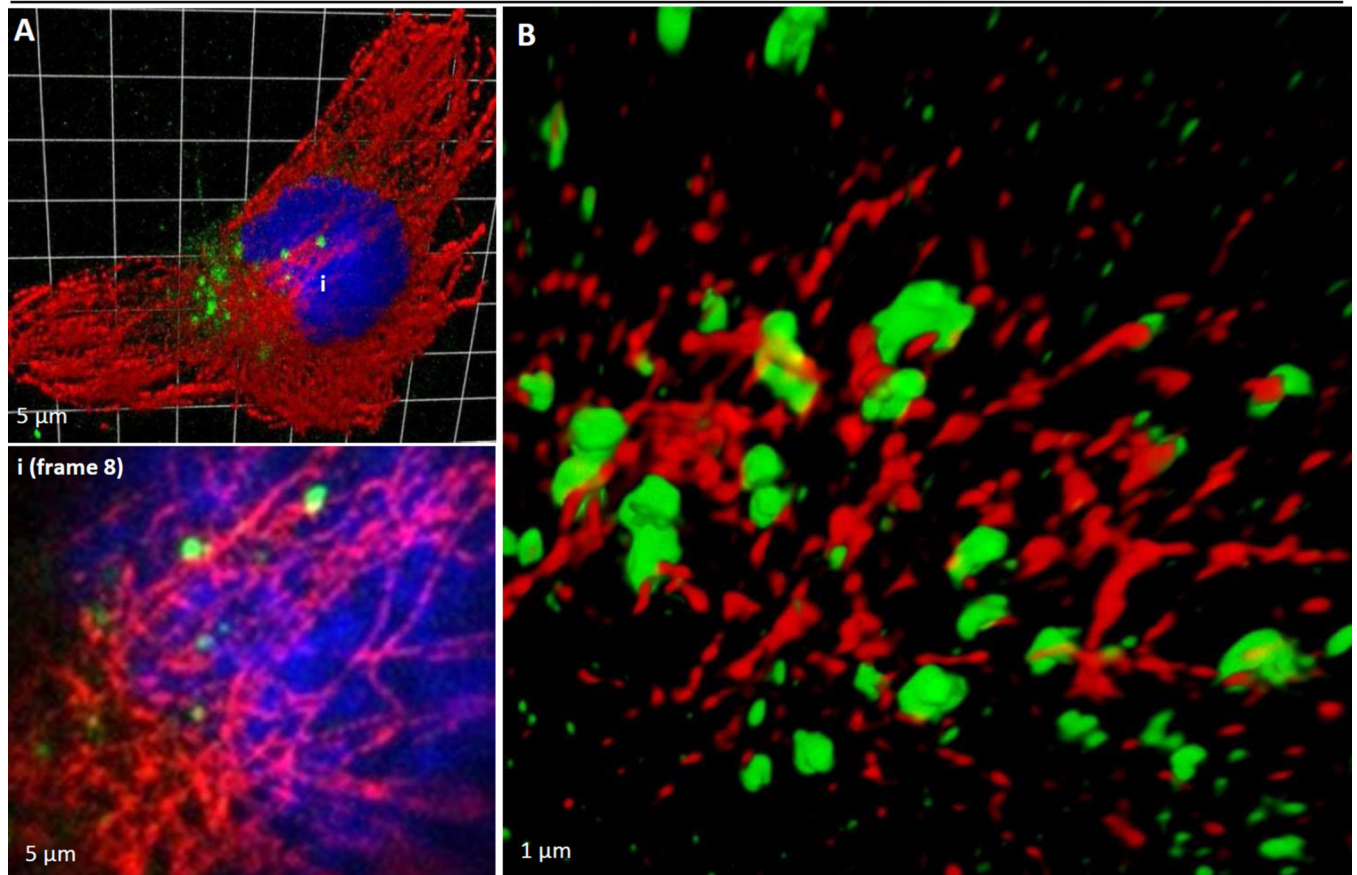


Fig. 4. TM4SF1 internalization along microtubules. HUVEC pre-labeled with 8G4 at 4°C and returned to culture at 37°C were harvested at 4h for immunostaining. 8G4 (green) and α -tubulin (red) immunofluorescence signals co-localized. (A) Z-stacked confocal image (27-stacks; 220 nm/stack) and a representative higher-resolution stack-8 image (inset i) show that internalized 8G4 is closely associated with α -tubulin stained microtubules. (B) Super-resolution Structured Illumination Microscopy demonstrate 8G4 signals in association with α -tubulin stained microtubules.